This article is available in PDF-format, in colour, at:
https://wydawnictwa.ipo.lukasiewicz.gov.pl/hig-en-mat-vol/vol-16-2/?lang=en

Materiały Wysokoenergetyczne / High Energy Materials, **2024**, *16*: 89 − 98; DOI 10.22211/matwys/0254
ISSN 2083-0165

Research paper / Praca doświadczalna

Mobile stand for static rocket motor testing
Mobilne stanowisko hamowni statycznej do badania silników rakietowych

Maciej Kołodziej*), **Jan Kindracki**, **Łukasz Mężyk**, **Sylwia Kozłowska**, **Krzysztof Wacko**, **Przemysław Woźniak**

Warsaw University of Technology, Faculty of Power and Aeronautical Engineering, Institute of Heat Engineering, 21/25 Nowowiejska Street, 00-665 Warsaw, Poland
** E-mail:* maciej.kolodziej.dokt@pw.edu.pl

ORCID Information:
Kozłowska S.: 0000-0002-8269-2340
Kindracki J.: 0000-0002-3453-7776
Woźniak P.: 0000-0002-1952-0343
Wacko K.: 0000-0002-6128-6730
Musky Ł.: 0000-0002-2297-5672
Kołodziej M.: 0000-0002-6765-6157

Abstract: *This paper presents the design and study of solid propellant rocket motors using a mobile test stand. The test stand allows the measurement of two primary rocket motor parameters: combustion chamber pressure and thrust. In addition, the measurement system is structured so that measurements other than those previously mentioned can be defined and implemented by the user. Each experiment is recorded with an industrial surveillance cameras system and a high-speed digital camera synchronised with the other data acquisition channels. So far, tests have been conducted on two different calibres of motor, each acting as the main motor in the rocket test platform. The tests confirmed the functionality of the described stand and its flexibility in adapting to users' requirements.*

Streszczenie: *W pracy przedstawiono projekt i badania wykonywane z wykorzystaniem mobilnego stanowiska do testów na hamowni silników rakietowych na stały materiał pędny, o kalibrach do 122 mm. Umożliwia ono pomiar dwóch podstawowych parametrów silnika rakietowego: ciśnienia w komorze spalania oraz generowanego ciągu. Dodatkowo, system pomiarowy jest zbudowany w sposób umożliwiający zdefiniowanie i zaimplementowanie przez użytkownika, pomiarów wielkości innych niż wspomniane. Każdy eksperyment jest nagrywany systemem kamer przemysłowych i szybką kamerą cyfrową zsynchronizowaną z pozostałymi kanałami pomiarowymi. Dotychczas eksperymenty prowadzono na dwóch różnych kalibrach silnika, każdy z nich spełniał rolę silnika głównego w rakietowej platformie testowej. Wykonane testy potwierdziły funkcjonalność opisanego stanowiska i jego elastyczność w dopasowaniu do wymagań użytkownika.*

Keywords: *static test stand, rocket motor, solid propellant, thrust measurement*
Słowa kluczowe: *hamownia statyczna, silnik rakietowy, stały materiał pędny, pomiar ciągu*

1. Introduction

The use of rocket motors has intensified due to the increasing ease of access to space by private companies [1] and their widespread use in combat [2, 3]. For spaceflight, the vast majority use liquid propellant engines or any type of gas engine [4] or by utilising electricity for propulsion. In the military use of these propulsion systems, the overwhelming majority are solid propellant motors. Being able to store them for many years in a condition that enables them to be quickly placed in combat readiness is a key factor [5, 6]. Another factor enabling their mass use as combat resources is their relatively low price and simplicity of operation [7]. These last two requirements make the design process particularly important, determining the success or otherwise of the design. In the course of the development of any rocket motor, tests on a static firing test stand play a key role, serving to confirm the parameters of the design experimentally, not only in terms of its strength but, above all, to provide data on the course of combustion chamber pressure and thrust during a motor's operation. It is also possible to use a range of other sensors to monitor the operating status of the entire structure, including temperature sensors, strain gauges, etc.

The test stand also allows testing to be carried out at the extreme temperatures required by the end user [8]. This makes it possible to study the effects of temperature on the combustion rate of the propellant and, consequently, the maximum pressure and thrust values during a motor's operation [9]. This data is extremely important regarding structural safety, as well as for modelling the flight dynamics of the missile. For rocket motors, there are two methods for measuring thrust: a direct method, where the thrust acts directly on a force sensor [10-12], and an indirect method called a 'baffle plate' using a plate affected by the exhaust gases which transmit forces to the sensor [13]. In the case of solid propellant motors, the first method is most commonly used due to the high temperatures of the exhaust gases and their corrosive properties caused by metal oxides or chlorine compounds. This article presents the design of a mobile motor test stand and describes its use in carrying out static firing tests.

2. Research stand

The stand was designed as a mobile carriage with a motor mounting bed, seated on rails in a rigid frame made of hollow stainless steel profiles (Figure 1). Welded joints integrated the individual profiles, and the finished structure was fitted with a resistance plate. The rigid rack is a 990×400 mm frame constructed from 40×40 mm square steel profiles. The integrated resistance plate is used to mount the force sensor, enabling the transfer of the force from the carriage to the rest of the stand, i.e. the foundation or T-table on which it is seated. The stand can be installed in a typical test stand building or in a shipping container capable of acting as a test stand building. Minimal displacement of the carriage is achieved by allowing it to move on polyamide rollers along the aforementioned slides. On the left side, the carriage is terminated with a steel plate to allow the installation of a force sensor bolted to a resistance plate on the other side. It is possible to use different types of force sensors on the stand, the installation of which is carried out via suitable mechanical interfaces. The stand described here uses a WObit force sensor bolted to the carriage plate and resistance plate, simultaneously providing a pre-load. It should be noted that the motor under test is mounted centrally in relation to the force sensor, thereby eliminating measurement errors that occur as a result of non-central mounting. Another important measurement carried out on the test stand is the measurement of the operating pressure in the combustion chamber. For this purpose, a Keller pressure sensor, type PAA-23SY, was used, with a range adapted to the anticipated motor operating parameters, i.e. 0-200 bar. The sensor has a ¼' (6.35 mm) connection, which is protected by a layer of special paste that thermally insulates the sensor from the hot gas stream. This solution allows it to be connected from the so-called bottom plug side of the motor. As mentioned earlier, the stand also allows additional measurements, such as the surface temperature of the motor body walls.

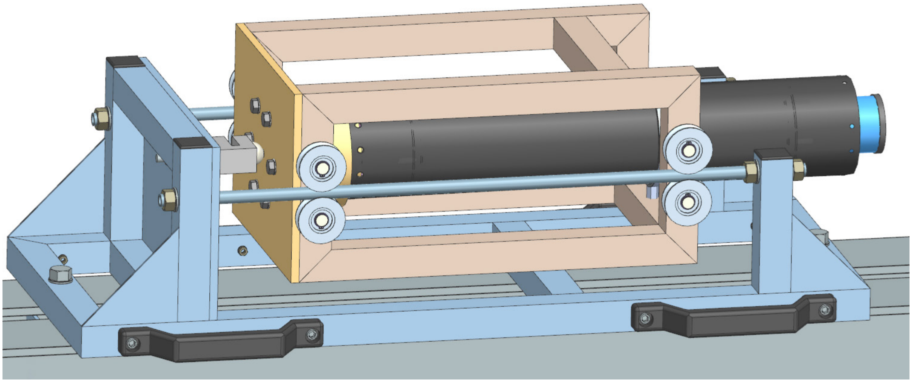

Figure 1. CAD model of test stand design

The measurements' accuracy largely depends on the measurement error (most commonly linearity error, zero tolerance, or hysteresis error) of the sensor used. In the case described here, a WObit sensor from the KMM 1503 series was used, with a measuring range of 0-10 kN and an estimated error of ±2%. Another important factor influencing accuracy when using strain gauges is the signal amplifier and the quality of the supply voltage. In the case described, the amplifier was made in-house using a calibrated reference voltage to reduce noise levels. The selection of the amplifier gain and the measuring range of the measuring card, 0-10 V, allows maximum error compensation. Figure 2 shows a diagram of the measurement system. In addition to the previously mentioned sensors, a National Instruments measurement card is included. This setup uses a convenient USB interface and a USB 6259 card with 8 analog channels, allowing a maximum measurement frequency of 125 kHz per channel. In the study, measurements were made at 50 kHz. The card also has digital channels to control external devices, such as an ignition system, or to activate a set of cameras recording a motor's operation. The operation of the measurement card is managed by in-house software written using libraries supplied by the manufacturer, National Instruments. For video recording, a set of Dahua IPC-HFW1431S-0280B-S4 industrial surveillance cameras is used, along with a high-speed digital camera from Photron SA 1.1, which can record up to 600 000 frames per second (fps). Studies typically utilize speeds of up to 5000 fps at a resolution of 1024×1024 using a telephoto lens.

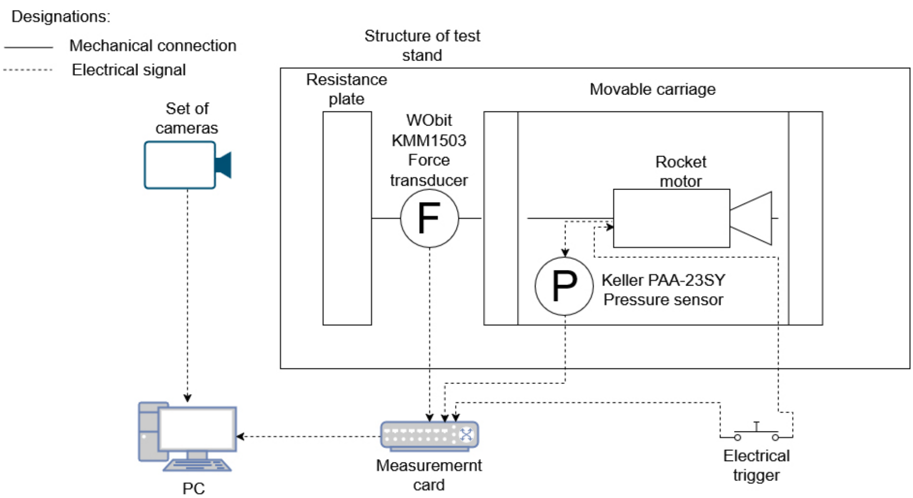

Figure 2. Diagram of the measurement system on the motor test stand

Table 1. Set of sensors used on the test stand

Sensor type	Manufacturer's designation	Measurement range
Pressure transmitter	Keller PAA-23SY	0-200 bar
Strain gauge transducer	WObit KMM1503	0-10 kN

3. Methodology of measurement

The thrust measurement is carried out on the test stand using the direct method, recording the force exerted by a motor's operation on the resistance face [11, 12]. In the chosen measurement method, the value of the force indicated by the sensor is, ideally, only the algebraic sum of the thrust and force from the sensor mounting. The value of the preload force can be determined individually from data obtained just prior to the motor starting to operate. To evaluate accurately the influence of various factors on the proposed method of measurement, other elements, shown in Equation 1, must also be taken into account.

$$F_{\mathrm{measured}} = F_{\mathrm{thrust}} + \Delta F_{\mathrm{fix}} + \Delta F_{\mathrm{T}} + \Delta F_{\mathrm{g}} + \Delta F_{\mathrm{PT}} + \Delta F_{\mathrm{i}} + \Delta F_{\mathrm{O}} \tag{1}$$

where: F_{thrust} – actual thrust value, ΔF_{fix} – correction for preload between sensor and structure, ΔF_{T} – error caused by the static friction of the rollers on the slides, ΔF_{g} – error caused by levelling errors, component from gravity, ΔF_{PT} – difference in motor thrust between ground test and flight operation at variable ceilings and in the presence of acceleration, ΔF_{i} – error caused by the sensor's reaction time, ΔF_{O} – error caused by ambient conditions (background vibrations).

The geometric and environmental conditions and the operating profile of the motor for a solid propellant of the sizes under test make thrust measurements on a test stand a relatively uncomplicated issue, as most of the errors mentioned are of a very small amplitude compared to the amount of thrust generated. The use of polyamide rollers allows movement along the slides with minimal friction. Tests carried out during the construction phase of the stand provided evidence for considering this factor negligible. The terms in Equation 1 relating to the influence of gravity and ambient vibrations of the test stand can also be ignored due to the ratio of their value to that of the generated force. The error associated with gravity for these motors can also be eliminated by ensuring horizontal leveling. The last term in the equation relates to environmental interference, mainly mechanical vibration. This is difficult to estimate because simultaneous thrust oscillations can occur, caused by micro-voids or, in the initial phase of measurement, by non-uniform ignition of the entire grain, making it impossible to separate the two. This component can also be omitted on the assumption that the data will be filtered during postprocessing, thus negating the effect of both sources. The processed data describes a smoothed, averaged thrust waveform. In view of this, Equation 1 is reduced to Equation 2.

$$F_{\mathrm{measured}} = F_{\mathrm{thrust}} + \Delta F_{\mathrm{fix}} \tag{2}$$

4. Experimental tests

This section of the paper discusses two example experiments on two different designs with 70 and 122 mm calibers. Both motors power the Warsaw University of Technology's rocket test platforms. The first platform – the RPT Artemida – used the Kallisto motor. The motor is 330 mm long, has an interchangeable nozzle, and can therefore be elaborated with various propellant grains, weighing approximately 1 kg, depending on the test requirements. The Syriusz motor for the second platform, the RPT Orion, is 676 mm long and contains approximately 5.5 kg of propellant based on ammonium chlorate(VII), HTPB, aluminum, and various additives necessary to regulate the rate of combustion or the crosslinking time of the grain. Both motors are designed to bind the grain to the wall through a thermal bonding layer, and the combustion surface is limited to the shape of the inner channel and the end cross-section of the grain on the nozzle side.

Prior to testing on a static test stand, a non-destructive test should be carried out for each motor to determine whether the propellant grain has internal defects that eliminate it from the test [14]. Two X-ray photographs per piece were taken for the large grain Syriusz motor or an X-ray CT scan in the case of the smaller Kallisto motor.

Figure 3 shows a normal grain image (Figure 3(a)) and a grain image with internal defects (Figure 3(b)) that made the test impossible. The propellant defects visible on X-ray images fall into two categories:

– Superficial:- cracks and fissures, often formed in the area of the core occupying the central channel; their presence can be caused by the temperature value at which the cross-linking of the material takes place,
– Sub-surface: gas bubbles trapped inside the grain volume could not be removed during the propellant elaboration process.

Defects of both types were noted in the grain in question. Their presence poses the risk of an uncontrolled increase in pressure in the combustion chamber, which can lead to a mechanical failure of the motor's body.

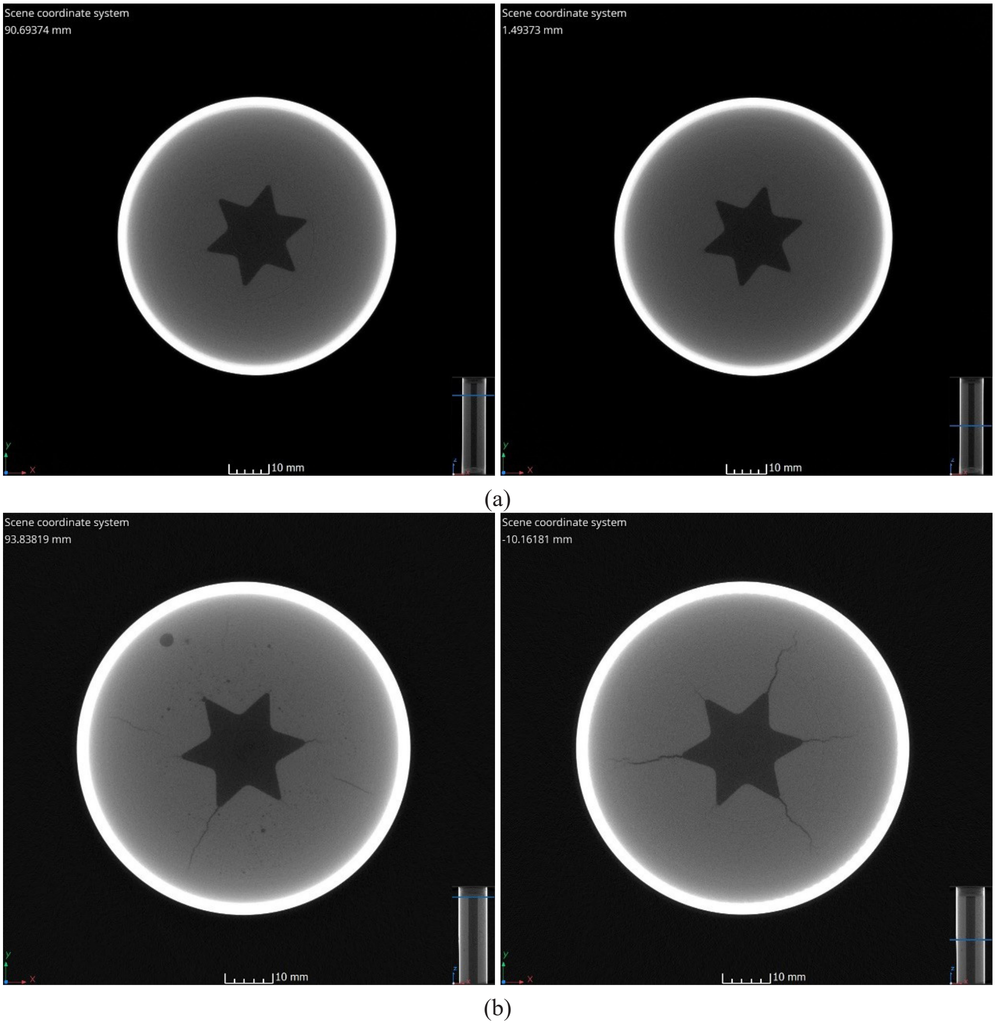

Figure 3. Example photos of non-destructive testing of propellant grains: a) grains approved for static firing test (a) and grains not approved for testing (b)

After non-destructive testing and a positive result, the propellant grain can be approved for static firing on a test stand. Figure 4 shows the data recorded during tests on the Syriusz motor test stand, during which, in addition to thrust and pressure, the temperature was measured at three points: on the body wall at a distance of 60 mm from the motor end section on the side of the bottom plug (T2), on the body wall at a distance of 85 mm from the motor end section on the side of the nozzle (T1) and the outer surface of the nozzle, near the exit section (T3). The pressure and thrust waveforms suggest that the ignition generated sufficient combustion gases needed to initiate the grain combustion process. However, breaking the nozzle plug quickly resulted in a sharp pressure drop. However, this did not lead to the motor stalling; the pressure again rose to the expected value, and the combustion process continued uninterrupted until the end. In this test, the aforementioned thermocouples were installed at two points on the body and the nozzle. They showed an expected gradual increase in the temperature of the outer wall of the body and nozzle, even after the combustion process (inertia of heat flow), not exceeding 100 °C. This indicates that the structure will not be at risk of overheating during operation, especially given that the body will be cooled by the jet of air washing over it during flight operations.

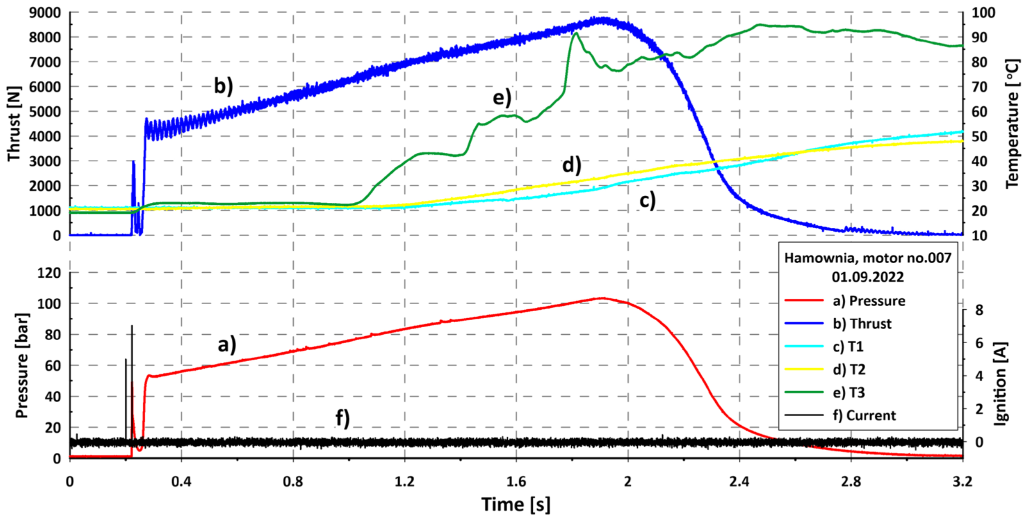

Figure 4. The waveform of measured parameters on the stand for the Syriusz motor, 122 mm calibre

(a)

(b)

Figure 5. A frame of the test run recorded with: an industrial camera positioned at the front above the motor (a) and a high-speed camera positioned at the side of the motor (b)

The waveform of example measured parameters for the Kallisto motor is shown in Figure 6. In the case of this motor, the ignition initiation went smoothly, the combustion process occurred as expected, and the slight overpressure at the beginning can be attributed to a slightly excessive mass of the powder charge used in the igniter. The pressure and thrust waveforms are relatively smooth, confirming that the motor was operating steadily and the grain did not contain void bubbles significant in size. No smoke can be seen in the images shown (Figure 7) for the Kallisto motor because a reduced-smoke propellant based on the energy polymer GAP was used for the tests.

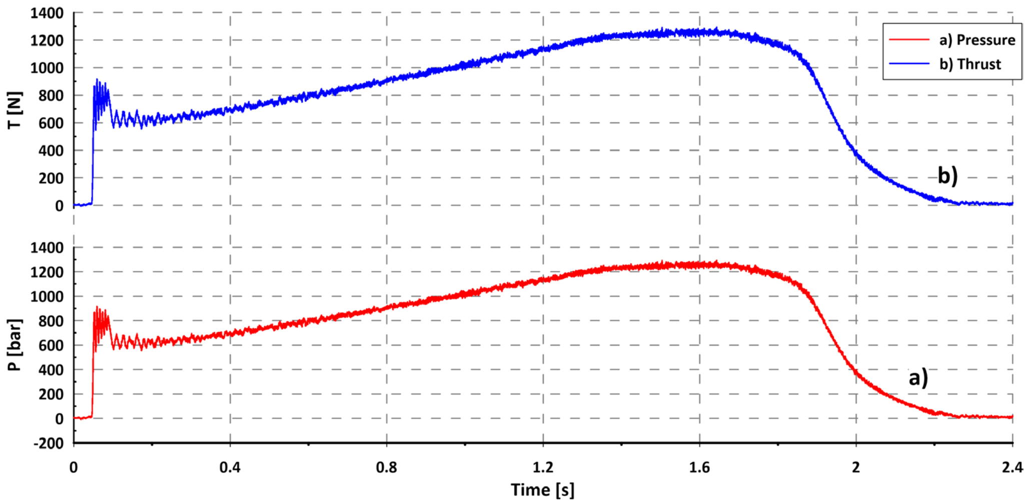

Figure 6. The waveform of measured parameters on the stand for the Kallisto motor, 70 mm calibre

Figure 7. Frames from a test run recorded with industrial cameras from two different angles

5. Summary and conclusions

The presented mobile test stand for the static firing of rocket motors up to 122 mm caliber and a maximum thrust of 10 kN has been designed for flexibility of use as the main goal. Its mobility allows it to be installed in a test building, but also to be carried to other sites at short notice, e.g. on an open-air testing facility. Currently, the limitation is the amount of thrust generated by the motor and the size of the motor caliber, but the stand can be scaled up, considering the need for appropriate safety factors. In the current solution, this is 10 kN, which provides a sufficiently large safety margin. Two basic parameters can be measured, namely combustion chamber pressure and thrust, with the installation of additional instrumentation, depending on the user's requirements. The measurements shown from two different locations, on a stationary test stand and in a shipping container, demonstrate the mobility of the test stand and its usability while ensuring the quality of the data obtained. The requirement for non-destructive measurements to check the quality of a propellant's elaboration minimizes the risk of motor damage or even explosion. The study shows that having a mobile test stand for testing the thrust of a rocket motor enables tests to be carried out at different locations, e.g. in a building (test stand building), on a training ground, or on a suitable field airfield, which can significantly reduce the cost of developing subsequent versions of a motor.

Acknowledgments

The presented research was funded by the National Centre for Research and Development under contract No. DOB-SZAFIR/03/B/001/01/2021, 'Development of a rocket motor based on unconventional fuel with reduced smoke and high specific impulse', as well as contract No. DOB-SZAFIR/03/B/002/01/2021, 'Development of a gas-dynamic control module for precise guidance of a missile', under the programme 'Development of modern, breakthrough technologies for national security and defence' – SZAFIR 1.

References

[1] Matthew Weinzierl M., Sarang M. The Commercial Space Age is Here. *Harvard Business Review* **2021**; https://hbr.org/2021/02/the-commercial-space-age-is-here [retrieved 22.10.**2024**].
[2] DeLuca L.T. Innovative Solid Formulations for Rocket Propulsion. *Eurasian Chem.-Technol. J.*

2016, *18*(3): 181-196; https://doi.org/10.18321/ectj42.

[3] Gok M.G., Cihan O. Energetic Materials and Metal Borides for Solid Propellant Rocket Engines. *IJMET* **2020**, *3*(2): 109-119; http://dergipark.gov.tr/tijmet.

[4] de Iaco Veris A. *Fundamental Concepts of Liquid -Propellant Rocket Engines*. 1st ed., Cham: Springer, **2021**; ISBN: 9783030547035.

[5] Lee D.N., Cho J.Y. Simplified Stochastic Temperature Model for Storage Reliability Estimation of Solid Rocket Propellants. *JMST* **2023**, *37*(1): 411-425; https://doi.org/10.1007/s12206-022-1239-7.

[6] Wang J., Cao P., Wang X. Review of the Mechanical Properties and Numerical Simulation of Composite Solid Propellants *Materials* **2023**, *16*(21) paper 6875; https://doi.org/10.3390/ma16216875.

[7] Singh H., Shekhar H. *Solid Rocket Propellants: Science and Technology Challenges*. The Royal Society of Chemistry, **2016**; ISBN 978-1-78262-096-9.

[8] Decner A., Polak A. Modern Test Stands and Dynamometers Equipped with Virtual and Traditional Measuring Instruments. (in Polish) *Napędy i Sterowanie* **2020**, *22*(6): 45-49.

[9] Sutton G.P., Biblarz O. *Rocket Propulsion Elements* 7th ed., New Delhi: Wiley India Pvt. Ltd., **2001**; ISBN 978-81-265-257-5.

[10] Hunt A., Cross A. *Guide to the Measurement of Force.* London: Institute of Measurement and Control, **1998**; ISBN: 0-904457-28-1.

[11] Lu J., Zheng L., Wang Z., Peng Ch., Cheng X. Thrust Measurement Method Verification and Analytical Studies on a Liquid-fueled Pulse Detonation Engine. *Chinese J. Aeronaut.* **2014**, *27*(3): 497-504; https://doi.org/10.1016/j.cja.2014.04.001.

[12] Jun Z., Akbar M.A., Lei W.X., Hua C.Y., Danaish, Theoretical and Experimental Investigation of Six-Degree-of-Freedom Force/Thrust Measurement Stand. *IET Sci. Meas. Technol.* **2020**, *14*(8): 883-890; https://doi.org/10.1049/iet-smt.2020.0046.

[13] Böhrk H., Auweter-Kurtz M. TIHTUS Thrust Measurement with a Baffle-Plate. *Proc. 43rd AIAA/ASME/SAE/ASEE Joint Propulsion Conference & Exhibit.* Cincinnati, US-OH, **2007**; https://doi.org/10.2514/6.2007-5297.

[14] Muralidhar C., Lukose S.N., Subramanian M.P., Reddy M.V., Joshi J.R. Evaluation of Internal Details in Rocket Motors Using Computed Tomography. *Proc. Indian National Sem. Exhib. Non-Destructive Evaluation (NDE2009)*, Tirichurappalli, India, **2009**, pp. 79-80.

Received: October 25, 2024
Revised: December 01, 2024
First published on line: December 20, 2024